SELECTIVE RETINAL THERAPY WITH MICROSECOND EXPOSURES USING A CONTINUOUS LINE SCANNING LASER

YANNIS M. PAULUS, MD,* ATUL JAIN, MD,* HIROYUKI NOMOTO, MD, PHD,* CHRISTOPHER SRAMEK, PHD,† RAY F. GARIANO, MD, PHD,* DAN ANDERSEN, BS,‡ GEORG SCHUELE, PHD,‡ LOH-SHAN LEUNG, MD, MS,* THEODORE LENG, MD,* DANIEL PALANKER, PHD*†

Purpose: To evaluate the safety, selectivity, and healing of retinal lesions created using a continuous line scanning laser.

Methods: A 532-nm Nd:YAG laser (PASCAL) with retinal beam diameters of 40 μm and 66 μm was applied to 60 eyes of 30 Dutch-belted rabbits. Retinal exposure duration varied from 15 μs to 60 μs. Lesions were acutely assessed by ophthalmoscopy and fluorescein angiography. Retinal pigment epithelial (RPE) flatmounts were evaluated with live–dead fluorescent assay. Histological analysis was performed at 7 time points from 1 hour to 2 months.

Results: The ratios of the threshold of rupture and of ophthalmoscopic visibility to fluorescein angiography visibility (measures of safety and selectivity) increased with decreasing duration and beam diameter. Fluorescein angiography and live–dead fluorescent assay yielded similar thresholds of RPE damage. Above the ophthalmoscopic visibility threshold, histology showed focal RPE damage and photoreceptor loss at 1 day, without inner retinal effects. By 1 week, photoreceptor and RPE continuity was restored. By 1 month, photoreceptors appeared normal.

Conclusion: Retinal therapy with a fast scanning continuous laser achieves selective targeting of the RPE and, at higher power, of the photoreceptors without permanent scarring or inner retinal damage. Continuous scanning laser can treat large retinal areas within standard eye fixation time.

RETINA X:1–9, 2010

Since its introduction nearly 40 years ago, laser photocoagulation remains the standard of care for many retinopathies.[1,2] By destroying retinal cells, panretinal laser photocoagulation is assumed to reduce metabolic demand to match the poor perfusion of ischemic retina. Production of hypoxia-inducible angiogenic factors is thereby reduced and retinal neovascularization regresses.[3–6] Because photoreceptors are the most numerous and metabolically active cells in the retina (containing large numbers of mitochondria), the therapeutic effect of panretinal laser photocoagulation in ischemic diseases, such as proliferative diabetic retinopathy, is likely achieved by the destruction of a fraction of the photoreceptors, without needing to damage the inner retina.

In conventional retinal photocoagulation, pulse durations are typically from 100 milliseconds to 200 milliseconds, laser spot diameters are from 100 μm to 500 μm, and powers range from 100 mW to 750 mW.[7–9] These parameters produce ophthalmoscopically visible gray–white lesions because of the thermal denaturation (coagulation) of photoreceptors and the inner retina. Heat is produced by light

From the *Department of Ophthalmology, Stanford University School of Medicine, Stanford, California; †Hansen Experimental Physics Laboratory, Stanford, California; and ‡OptiMedica Inc, Santa Clara, California.

Funding was provided in part by the Alcon Research Institute, the Horngren and Miller Family Foundations, OptiMedica, Corp, Air Force Office of Scientific Research, the Heed Ophthalmic Foundation, and the Angelos and Penelope Dellaporta Research Fund.

D. Andersen and G. Schuele are employees of OptiMedica Corporation.

D. Palanker holds a Stanford University patent on patterned scanning laser photocoagulation licensed to OptiMedica Corporation with an associated equity and royalty interest and serves as a consultant for OptiMedica Corporation.

Reprint requests: Yannis Paulus, MD, Eye Institute at Stanford, 2452 Watson Court, Palo Alto, CA 94303-5353; e-mail: ypaulus@stanford.edu

COLOR

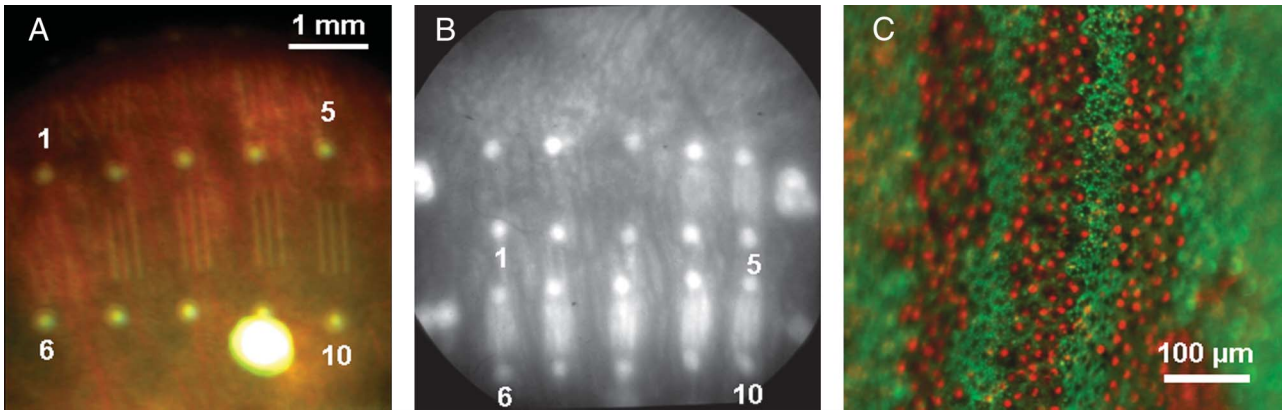

Fig. 1. Determination of ophthalmoscopic visibility, angiographic visibility, and live–dead staining thresholds of the retinal lesions. Sets of three lines are placed in a grid of increasing power (from top left to bottom right) with visible marker burns to facilitate localization. Sets of lines are referred to from 1 in the top left to 10 in the bottom right. **A.** Fundus photograph showing marker burns and patterns of 3 lines applied at increasing laser power. Ophthalmoscopic visibility threshold power is at the lesion 7. **B.** FA photograph showing marker spot lesions and 2 rows of line patterns of increasing laser power. The first three sets of lesions in the top row (1–3) are angiographically invisible; lesion 4 indicates angiographic threshold. **C.** Retinal pigment epithelium wholemount stained with LIVE/DEAD fluorescent assay, showing dead cells (red) within linear laser lesions.

nucleic acid stain to label all cells and a DEAD Red (ethidium homodimer-2) nucleic acid stain to label only cells with compromised cell membranes. The animals were killed 1 hour after laser application; the eyes were enucleated and the anterior portion (lens, cornea, and anterior chamber) was dissected away. The vitreous was then removed, and the irradiated portion of the retina, RPE, choroid, and sclera was sectioned. The retina was then gently peeled away from the RPE, and the fluorescent stain was placed directly on the RPE. These sections were incubated in a humid chamber for 20 minutes at room temperature, whereupon they were imaged on an inverted fluorescent microscope.

Statistical Analysis

The ED_{50} is the median effective dose, or the laser power required to produce the specific effect in 50% of the measurements, with the specified effects including FA visibility, ophthalmoscopic visibility, and rupture of Bruch's membrane. The ED_{50} measurements were made with a probit analysis using StatPlus (AnalystSoft, Vancouver, Canada) to calculate the thresholds in 4 to 8 eyes with 1 to 2 patterns per eye for each threshold measurement. The ED_{50} values were calculated to a minimum of 3 significant figures, and the ratios of the threshold values were thus also calculated to 3 significant figures.

Results

Thresholds Determination

The thresholds for rupture of Bruch's membrane, ophthalmoscopic and FA visibility, and live/dead assay were determined for beam sizes of 40 μm and 66 μm and dwell times of 15 microseconds and 60 microseconds. Figure 1 demonstrates the appearance of the line patterns using these techniques. Patterns included 10 groups of 3 lines in each, arranged in 2 rows, with conventional spot marker lesions in between. Laser power increases between these 10 groups from left to right and from top to bottom. In an example shown in Figure 1A, the bottom 4 lesions from the right (numbers 7–10) are visible ophthalmoscopically. With FA, the bottom 5 and the top 2 lesions on the right (numbers 4–10) are visible (Figure 1B). A higher magnification image of the 3-line pattern stained with live/dead assay is shown in Figure 1C.

Table 1. Threshold of Angiographic and Ophthalmoscopic Visibility and Rupture

Beam Size (μm)	Dwell Time (μs)	ED50 FA (mW)	ED50 Ophthal (mW)	ED50 Rupture (mW)	Ophthal/FA	Rupture/Ophthal	Rupture/FA
40	15	375 ± 146	1,043 ± 227	2,263 ± 206	3.10 ± 1.38	2.09 ± 0.13	7.16 ± 2.69
40	60	131 ± 43	216 ± 37	988 ± 48	1.81 ± 0.81	4.53 ± 0.23	7.05 ± 0.96
66	15	500 ± 122	1,253 ± 205	2,600 ± 200	2.58 ± 0.53	2.32 ± 0.22	5.08 ± 0.45
66	60	280 ± 67	458 ± 121	1,260 ± 65	1.65 ± 0.37	2.76 ± 0.15	4.46 ± 0.25

Mean and standard deviations of the ED_{50} values for angiographic visibility, ophthalmoscopic visibility, and rupture for beam sizes of 40 μm and 66 μm and dwell times of 15 microseconds and 60 microseconds.

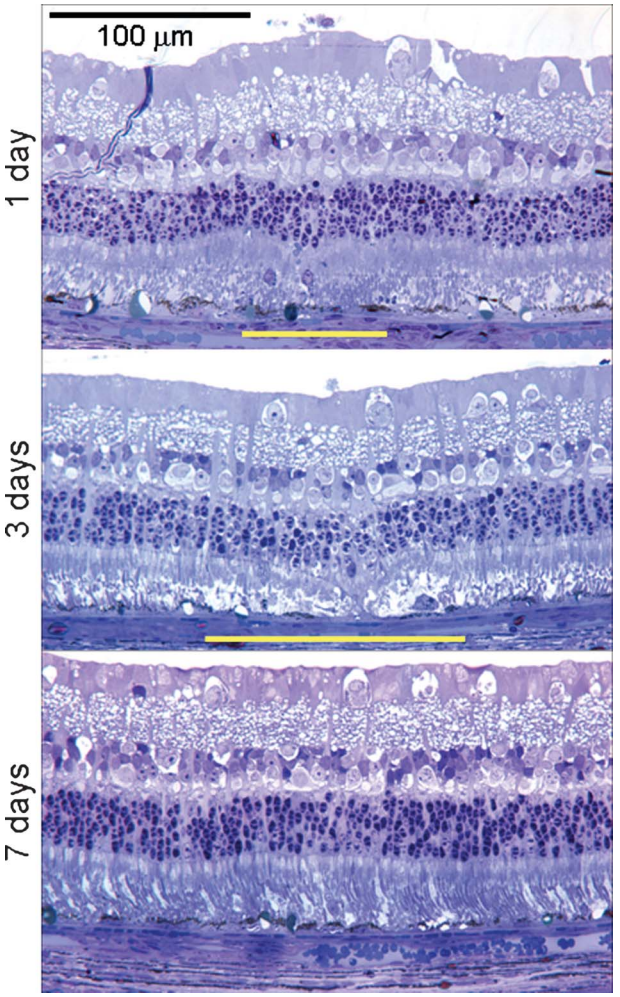

Fig. 2. Clinically invisible lesion at 1 day (**A**), 3 days (**B**), and 7 days (**C**) after treatment. Beam diameter 66 μm, dwell time 15 microseconds, and power 1,100 mW. All fundus photographs were taken with a ×20 microscope objective. One day demonstrates RPE cell collapse and increased density of the outer segments. At 3 days, outer segments appear abnormal within a zone twice wider than the initial lesion, with edema between the outer segments and RPE. By 1 week, the RPE defect and the damage to the outer segments have largely resolved.

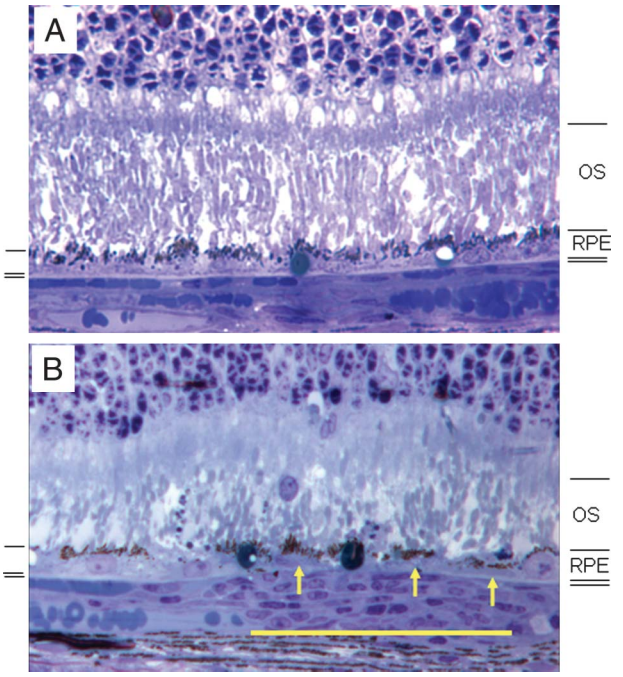

Fig. 3. Clinically invisible lesion at higher magnification (×40). **A.** Untreated retina demonstrating normal RPE–photoreceptor architecture. **B.** Retina at 1 day after laser treatment (clinically invisible, beam diameter 66 μm, 15 microseconds, and 1,100 mW). Retinal pigment epithelial cells collapse (yellow arrows) at the site of laser application (yellow line), and outer segments above them appear denser.

Measured thresholds of these visibility criteria and rupture are summarized in Table 1. The threshold of RPE damage is defined as ED_{50} level of the FA visibility. The ED_{50} for live/dead visibility corresponded exactly with that of FA ED_{50} (data not shown). The ED_{50} level of ophthalmoscopic visibility (OV) corresponds to the threshold of visible changes. Histologic analysis below demonstrated that this threshold corresponds to photoreceptor damage.

As expected, the ED_{50} for all thresholds increases with decreasing pulse duration. Because retinal rupture is an undesirable outcome, its threshold represents an upper limit of the safe dynamic range of the retinal treatment. The ratio of the threshold power for rupture to that of FA visibility defines the safe therapeutic window of this treatment. Smaller beam size (40 μm vs. 66 μm) resulted in a higher safety ratio: 7.16 versus 5.08 for 15-microsecond dwell time and 7.05 versus 4.46 for 60-microsecond dwell time ($P < 0.01$). Shorter exposures resulted in only a slight, statistically nonsignificant increase in the safe dynamic range: 7.05 versus 7.16 for a beam size of 40 μm and 4.46 versus 5.08 for a beam size of 66 μm for dwell times of 60 microseconds and 15 microseconds, respectively.

The treatment selectivity (i.e., RPE damage with sparing of photoreceptors) can be estimated as the ratio of the thresholds of OV to FA. In contrast to the safe therapeutic window, the dwell time markedly impacts lesion selectivity. Reducing the beam size from 66 μm to 40 μm resulted in minimal increase in the OV to FA ratio from 2.58 to 3.10 for 15-microsecond dwell time and from 1.65 to 1.81 for 60-microsecond dwell time. However, reducing dwell time from 60 microseconds to 15 microseconds resulted in a significant increase in the treatment selectivity, from 1.81 to 3.10 for 40-μm lesion size and from 1.65 to 2.58 for 66-μm lesion size ($P < 0.01$). Increasing the number of repetitions of the scan to 10 or 100 did not improve the safety window or the treatment selectivity (data not shown).

C
O
L
O
R

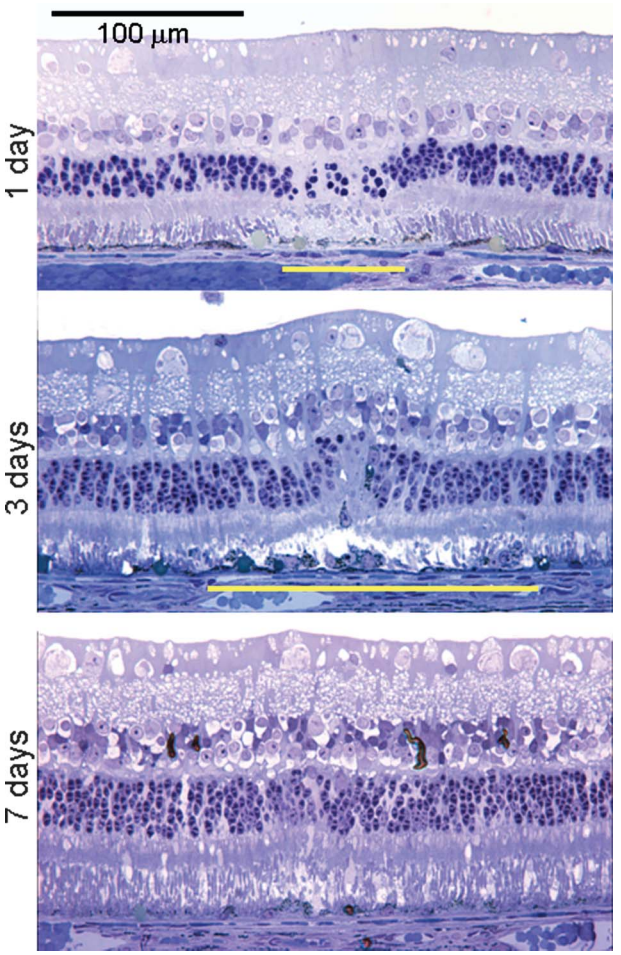

Fig. 4. Resolution of photoreceptor damage in the visible lesions. Dwell time 60 microseconds, laser power 1,000 mW, a single 66 mm line. Yellow bar indicates the extent of abnormal zone at the RPE–photoreceptor junction. Cellular loss is evident at 1 day in the ONL. The extent of nuclear dropout decreases at 3 days within the lesion; although the photoreceptor–RPE junction shows a widening of the area of disturbed, anatomy demonstrated loss of the vertical orientation of outer segments, edema between the inner and outer segments, and marked variability of the inner and outer segment thickness. At 7 days, a complete restoration of normal anatomy returns to both ONL and outer segments.

Healing of Retinal Line Lesions

Healing of retinal lesions produced by line scanning laser with microsecond exposures was followed over 2 months for both combinations of dwell times and beam sizes at 3 laser intensities. Representative lesions are shown in Figures 2–5.

In initially ophthalmoscopically invisible lesions at 1 day, RPE cells appear collapsed and outer segments appear more heavily stained with toluidine blue and increased in density (Figures 2 and 3). There is no evidence of loss of nuclei in the outer nuclear layer (ONL), although the photoreceptor outer segments do demonstrate disorganization. At 3 days, both above the original lesion and also in the adjacent initially unaffected areas, the outer segments appear in an oblique orientation, edema exist between outer segments and RPE, and the outer segment thickness shows marked variability. At 3 days, there is no evidence of photoreceptor death and nuclear loss for ophthalmoscopically invisible lesions (Figure 2), whereas this is noted for visible lesions (Figure 4). The average width of these ophthalmoscopically invisible lesions at 3 days was 118 μm (SD, 9.5 μm), which is twice the width of the laser beam. Photoreceptors regain their normal morphology by 1 week (Figure 2).

Visible lesions were associated with photoreceptor death within 1 day of treatment (Figures 4 and 5). These lesions exhibited cellular loss at 1 day, with pyknosis and reduced numbers of nuclei in the ONL, hypopigmentation of the inner and outer segments, heavier staining with toluidine blue at round foci at the inner segment/outer segment junction, oblique orientation of the outer segments, and some edema between the RPE and photoreceptors. The inner retina was well preserved at all periods. In the single line lesion (Figure 4), damage in the ONL decreases at 3 days and resolves by 7 days. However, the abnormality at the photoreceptor–RPE junction widens significantly at 3 days compared with the initial lesion width and then resolves by 7 days.

Placement of 3 adjacent line lesions separated by 2 beam diameters altered the healing dynamics remarkably (Figure 5). At 1 day, these lesions exhibited findings typical of single line lesions described above, that is, pyknosis and reduced numbers of nuclei in the ONL, minor displacement of the ONL into the photoreceptor (PR) inner segments, slight edema and retinal thickening at the site of the laser patterns. However, at 3 days a dramatic change is noted in the surrounding photoreceptor regions: the vertical orientation of the outer segments is replaced with a haphazard arrangement, edema exists between inner and outer segments, and inner and outer segment thickness shows marked variability. At the laser sites, the lesions show minimal pyknosis and greatly reduced numbers of nuclei in the ONL, increased displacement of the ONL into the PR inner segments, edema, and retinal thickening. By 2 weeks, continuity of the ONL and photoreceptor anatomy were restored. Small patches of RPE hypertrophy persist at 2 months (Figure 5, arrows), but relatively normal anatomy of the outer segments was restored. In addition, density of the inner and outer segments layers and ONL appeared decreased both within the region of laser exposure and in the surrounding 120 μm.

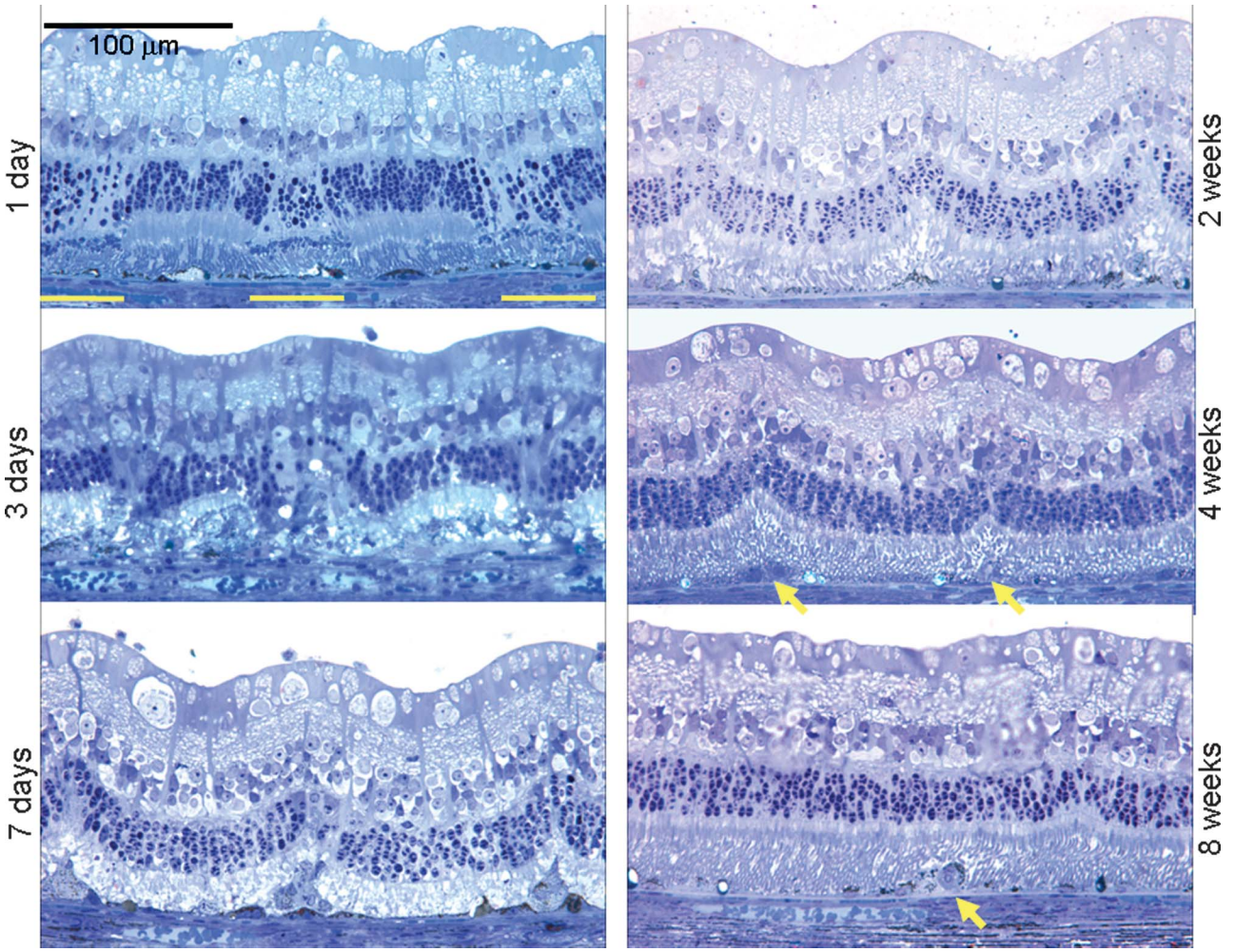

COLOR

Fig. 5. Healing dynamics of a three-line pattern with line separations of two beam diameters. The laser parameters are identical to Figure 4. At 1 day, there is pyknosis and nuclear dropout in the ONL. At 3 days, a dramatic change in normal anatomy is noted in the surrounding photoreceptor regions. By 2 weeks, nuclear continuity and photoreceptor anatomy are largely restored. The retina flattens by 2 months, while some RPE hypertrophy persists (yellow arrow).

Discussion

Retinal pigment epithelium dysfunction occurs in several macular diseases, including age-related macular degeneration, diabetic macular edema, and CSC. This suggests a need for RPE-specific therapies, which SRT can achieve with microsecond pulses or the rapid scanning of a continuous laser.[45,51]

We find that 15-microsecond and 60-microsecond retinal exposures produced by line scanning mode of the PASCAL laser damages the RPE without a loss of photoreceptors. Decreasing dwell time (increasing scanning speed) results in improved selectivity of the damage. As has been established previously,[14] the safe therapeutic window is defined by the maximum intensity divided by the minimum intensity required for a desired outcome while avoiding an undesirable side effect. Because angiographic visibility corresponds to RPE damage, and retinal rupture should be avoided, the therapeutic window for the treatment of RPE would be the ratio of the threshold power for rupture to that of FA visibility. Ophthalmoscopic visibility of the lesion corresponds to photoreceptor damage, and therefore therapeutic window of selective RPE treatment (aka, treatment that does not damage photoreceptors) is defined by the ratio of threshold powers for ophthalmoscopic and angiographic visibility. We find that a single line scanning approach (i.e., no repetitive scanning) provides a sufficiently large safety window of 4.5 to 7.2. For comparison, safe therapeutic window of conventional photocoagulation with 100-millisecond pulses is approximately 4.[14]

The dynamic range increased for decreasing exposure duration and also for decreasing lesion width. For our beam sizes (40 and 66 μm) and pulse durations (15 and 60 μs), reducing the beam diameter was the most efficient means to increase the therapeutic window. In contrast, selectivity of RPE

treatment, as determined by the ratio of OV to FA, was improved more by decreasing the dwell time.

Even if the threshold of ophthalmic visibility is exceeded, only relatively mild photoreceptor damage appears and it resolves without retinal scarring or gliosis within 1 week. Although lesions resulting from the dense patterns of three lines heal slower—perhaps because of more limited capacity of adjacent photoreceptors to migrate into lesions—by 2 months, photoreceptor continuity was restored in all cases, without scarring. These findings suggest that if the threshold of photoreceptor damage was inadvertently exceeded (e.g., because of pigmentation variation), permanent scars or scotomas would not ensue. This added safety is an attractive feature of microsecond laser for clinical use in the macula.

At 3 days after visible burn formation, mild abnormalities appear in the photoreceptor outer segments beyond the zone of RPE damage (Figure 4). This secondary effect of detaching and shortening of the outer segments from the underlying RPE may be because of proliferation and migration of surrounding RPE cells to restore continuity to the damaged area, which has been demonstrated to occur within one week.[15] Redistribution of the photoreceptors by lateral migration from the unaffected areas into the damage zone restores continuity of the photoreceptor layer, with ONL cell density slightly reduced adjacent to the lesions, as we observed. This rearrangement and depletion of photoreceptors is even more evident in dense patterns of multiple lines, as shown in Figure 5.

In contrast to a previous study by Framme et al,[45] we do not find that multiple scans improve the safety or selectivity of the treatment. This difference could be because of the greater role of thermal diffusion and heat accumulation in our approach because it involves larger beam size (40 and 66 vs. 18 μm) and longer exposures (15 and 60 vs. 7.5 μs).

Selective treatment of RPE using a line scanning laser is a promising new modality characterized by enhanced selectivity and lack of permanent retinal structural sequelae. These features are particularly desirable when considering macular therapy. Moreover, a high beam velocity enables rapid treatment of relatively large retinal areas. For example, with a beam size of 60 μm, a 15-microsecond exposure time is achieved with a scanning velocity of 4 m/s. At such speed, 24 mm^2 can be treated within 100 milliseconds. For comparison, the total coagulated area using the modified Early Treatment Diabetic Retinopathy Study or mild macular grid photocoagulation does not exceed 6 mm^2.[52] The entire macula can be treated with a line scanning laser within a time shorter than a single conventional exposure.

Key words: microsecond pulse duration, retinal laser photocoagulation, retinal pigment epithelium, scanning laser, selective retinal therapy.

Acknowledgments

The authors thank Roopa Dalal for histological preparations; Resmi Charalel for lesion size measurements, stimulating discussion, and assistance with animal care and handling; and Phil Huie for assistance with animal care and handling.

References

1. Kapany NS, Peppers NA, Zweng HC, Flocks M. Retinal photocoagulation by lasers. Nature 1963;199:146–149.
2. Little HL, Zweng HC, Peabody RR. Argon laser slit-lamp retinal photocoagulation. Trans Am Acad Ophthalmol Otolaryngol 1970;74:85–97.
3. Jennings PE, MacEwen CJ, Fallon TJ, Scott N, Haining WM, Belch, JJ. Oxidative effects of laser photocoagulation. Free Radic Biol Med 1991;11:327–330.
4. Matsumoto M, Yoshimura N, Honda Y. Increased production of transforming growth factor-beta 2 from cultured human retinal pigment epithelial cells by photocoagulation. Invest Ophthalmol Vis Sci 1994;35:4245–4252.
5. Sanchez MC, Luna JD, Barcelona PF, et al. Effect of retinal laser photocoagulation on the activity of metalloproteinases and the alpha(2)-macroglobulin proteolytic state in the vitreous of eyes with proliferative diabetic retinopathy. Exp Eye Res 2007;85:644–650.
6. Spranger J, Hammes HP, Preissner KT, Schatz H, Pfeiffer AF. Release of the angiogenesis inhibitor angiostatin in patients with proliferative diabetic retinopathy: association with retinal photocoagulation. Diabetologia 2000;43:1404–1407.
7. Early Treatment Diabetic Retinopathy Study Research Group. Treatment techniques and clinical guidelines for photocoagulation of diabetic macular edema. Early Treatment Diabetic Retinopathy Study report number 2. Ophthalmology 1987;94:761–774.
8. Smiddy WE, Fine SL, Quigley HA, Hohman RM, Addicks EA. Comparison of krypton and argon laser photocoagulation. Results of stimulated clinical treatment of primate retina. Arch Ophthalmol 1984;102:1086–1092.
9. Smiddy WE, Patz A, Quigley HA, Dunkelberger GR. Histopathology of the effects of tuneable dye laser on monkey retina. Ophthalmology 1988;95:956–963.
10. Birngruber R, Hillenkamp F, Gabel VP. Theoretical investigations of laser thermal retinal injury. Health Phys 1985;48:781–796.
11. Marshall J, Mellerio J. Pathological development of retinal laser photocoagulations. Exp Eye Res 1967;6:303–308.
12. Sramek C, Paulus Y, Nomoto H, Huie P, Brown J, Palanker D. Dynamics of retinal photocoagulation and rupture. J Biomed Opt 2009;14:034007.
13. Higgins KE, Meyers SM, Jaffe MJ, Roy MS, de Monasterio FM. Temporary loss of foveal contrast sensitivity associated with panretinal photocoagulation. Arch Ophthalmol 1986;104:997–1003.
14. Jain A, Blumenkranz MS, Paulus Y, et al. Effect of pulse duration on size and character of the lesion in retinal photocoagulation. Arch Ophthalmol 2008;126:78–85.
15. Paulus YM, Jain A, Gariano RF, et al. Healing of retinal photocoagulation lesions. Invest Ophthalmol Vis Sci 2008;49:5540–5545.

16. Shimura M, Yasuda K, Nakazawa T, Tamai M. Visual dysfunction after panretinal photocoagulation in patients with severe diabetic retinopathy and good vision. Am J Ophthalmol 2005;140:8–15.
17. Early Treatment Diabetic Retinopathy Study Research Group. Focal photocoagulation treatment of diabetic macular edema. Relationship of treatment effect to fluorescein angiographic and other retinal characteristics at baseline: ETDRS report no. 19. Arch Ophthalmol 1995;113:1144–1155.
18. Morgan CM, Schatz H. Atrophic creep of the retinal pigment epithelium after focal macular photocoagulation. Ophthalmology 1989;96:96–103.
19. Schatz H, Madeira D, McDonald HR, Johnson RN. Progressive enlargement of laser scars following grid laser photocoagulation for diffuse diabetic macular edema. Arch Ophthalmol 1991;109:1549–1551.
20. Lewen RM. Subretinal neovascularization complicating laser photocoagulation of diabetic maculopathy. Ophthalmic Surg 1988;19:734–737.
21. Lewis H, Schachat AP, Haimann MH, et al. Choroidal neovascularization after laser photocoagulation for diabetic macular edema. Ophthalmology 1990;97:503–510.
22. Guyer DR, D'Amico DJ, Smith CW. Subretinal fibrosis after laser photocoagulation for diabetic macular edema. Am J Ophthalmol 1992;113:652–656.
23. Lovestam-Adrian M, Agardh E. Photocoagulation of diabetic macular oedema—complications and visual outcome. Acta Ophthalmol Scand 2000;78:667–671.
24. Rutledge BK, Wallow IH, Poulsen GL. Sub-pigment epithelial membranes after photocoagulation for diabetic macular edema. Arch Ophthalmol 1993;111:608–613.
25. Hudson C, Flanagan JG, Turner GS, Chen HC, Young LB, McLeod D. Influence of laser photocoagulation for clinically significant diabetic macular oedema (DMO) on short-wavelength and conventional automated perimetry. Diabetologia 1998;41:1283–1292.
26. Ishiko S, Ogasawara H, Yoshida A, Hanada K. The use of scanning laser ophthalmoscope microperimetry to detect visual impairment caused by macular photocoagulation. Ophthalmic Surg Lasers 1998;29:95–98.
27. Mainster MA. Decreasing retinal photocoagulation damage: principles and techniques. Semin Ophthalmol 1999;14:200–209.
28. Sinclair SH, Alaniz R, Presti P. Laser treatment of diabetic macular edema: comparison of ETDRS-level treatment with threshold-level treatment by using high-contrast discriminant central visual field testing. Semin Ophthalmol 1999;14:214–222.
29. Striph GG, Hart WM Jr, Olk RJ. Modified grid laser photocoagulation for diabetic macular edema. The effect on the central visual field. Ophthalmology 1988;95:1673–1679.
30. Busch EM, Gorgels TG, Van Norren D. Filling-in after focal loss of photoreceptors in rat retina. Exp Eye Res 1999;68:485–492.
31. Zwick H, Edsall P, Stuck BE, et al. Laser induced photoreceptor damage and recovery in the high numerical aperture eye of the garter snake. Vision Res 2008;48:486–493.
32. Blumenkranz MS, Yellachich D, Andersen DE, et al. Semiautomated patterned scanning laser for retinal photocoagulation. Retina 2006;26:370–376.
33. Al-Hussainy S, Dodson PM, Gibson JM. Pain response and follow-up of patients undergoing panretinal laser photocoagulation with reduced exposure times. Eye 2008;22:96–99.
34. Muqit MM, Marcellino GR, Gray JC, et al. Pain responses of Pascal 20 ms multi-spot and 100 ms single-spot panretinal photocoagulation: Manchester Pascal Study, MAPASS report 2. Br J Ophthalmol 2010; Jun 16 [Epub ahead of print].
35. Nagpal M, Marlecha S, Nagpal K. Comparison of laser photocoagulation for diabetic retinopathy using 532-nm standard laser versus multispot pattern scan laser. Retina 2010;30:452–458.
36. Roider J, Michaud NA, Flotte TJ, Birngruber R. Response of the retinal pigment epithelium to selective photocoagulation. Arch Ophthalmol 1992;110:1786–1792.
37. Roider J, Hillenkamp F, Flotte T, Birngruber R. Microphotocoagulation: selective effects of repetitive short laser pulses. Proc Natl Acad Sci U S A 1993;90:8643–8647.
38. Roider J, Brinkmann R, Wirbelauer C, Laqua H, Birngruber R. Subthreshold (retinal pigment epithelium) photocoagulation in macular diseases: a pilot study. Br J Ophthalmol 2000;84: 40–47.
39. Framme C, Walter A, Prahs P, et al. Structural changes of the retina after conventional laser photocoagulation and selective retina treatment (SRT) in spectral domain OCT. Curr Eye Res 2009;34:568–579.
40. Lee H, Alt C, Pitsillides CM, Lin CP. Optical detection of intracellular cavitation during selective laser targeting of the retinal pigment epithelium: dependence of cell death mechanism on pulse duration. J Biomed Opt 2007;12: 064034.
41. Elsner H, Porksen E, Klatt C, et al. Selective retina therapy in patients with central serous chorioretinopathy. Graefes Arch Clin Exp Ophthalmol 2006;244:1638–1645.
42. Elsner H, Klatt C, Liew SH, et al. [Selective retina therapy in patients with diabetic maculopathy]. Ophthalmologe 2006; 103:856–860.
43. Brinkmann R, Roider J, Birngruber R. Selective retina therapy (SRT): a review on methods, techniques, preclinical and first clinical results. Bull Soc belge Ophtalmol 2006;302:51–69.
44. Friberg TR, Karatza EC. The treatment of macular disease using a micropulsed and continuous wave 810-nm diode laser. Ophthalmology 1997;104:2030–2038.
45. Framme C, Schuele G, Roider J, Kracht D, Birngruber R, Brinkmann R. Threshold determinations for selective retinal pigment epithelium damage with repetitive pulsed microsecond laser systems in rabbits. Ophthalmic Surg Lasers 2002;33: 400–409.
46. Roider J, Brinkmann R, Wirbelauer C, Laqua H, Birngruber R. Retinal sparing by selective retinal pigment epithelial photocoagulation. Arch Ophthalmol 1999;117:1028–1034.
47. Framme C, Alt C, Schnell S, Sherwood M, Brinkmann R, Lin CP. Selective targeting of the retinal pigment epithelium in rabbit eyes with a scanning laser beam. Invest Ophthalmol Vis Sci 2007;48:1782–1792.
48. Birngruber R. Choroidal circulation and heat convection at the fundus of the eye: implications for laser coagulation and the stabilization of retinal temperature. In: Wolbarsht ML, ed. Laser Applications to Medicine and Biology. Vol 5. New York, NY: Plenum Press; 1991: 277–362.
49. Turner KW. Hematoxylin toluidine blue-phloxinate staining of glycol methacrylate sections of retina and other tissues. Stain Technol 1980;55:229–233.
50. Maia M, Kellner L, de Juan E Jr, et al. Effects of indocyanine green injection on the retinal surface and into the subretinal space in rabbits. Retina 2004;24:80–91.
51. Framme C, Schuele G, Roider J, Birngruber R, Brinkmann R. Influence of pulse duration and pulse number in selective RPE laser treatment. Lasers Surg Med 2004;34:206–215.
52. Committee for the Diabetic Retinopathy Clinical Research Network. Comparison of the modified Early Treatment Diabetic Retinopathy Study and mild macular grid laser photocoagulation strategies for diabetic macular edema. Arch Ophthalmol 2007; 125:469–480.